

# Micromachined temperature calibration tool for contact Scanning Thermal Microscope probes

A. Bontempi<sup>1</sup>, T. P. Nguyen<sup>1</sup>, E. Lemaire<sup>2</sup>, L. Thiery<sup>1</sup>, D. Teyssieux<sup>1</sup>, S. Euphrasie<sup>1</sup>, D. Briand<sup>3</sup> and P. Vairac<sup>1</sup>

<sup>1</sup> FEMTO-ST, Université de Franche-Comté, CNRS, ENSMM, UTBM, Besançon, France

<sup>2</sup> Microsystems for Space Technologies Laboratory, EPFL, Neuchâtel, Switzerland

<sup>3</sup> The Sensors, Actuators and Microsystems Laboratory, EPFL, Neuchâtel, Switzerland

\* Corresponding author: laurent.thiery@univ-fcomte.fr,+33-370049026

## Abstract

Local thermal probing has become a major tool for studying transport phenomena at micro and nanoscale levels, detecting hot spots and failures of microelectronic devices or measuring surface temperature distribution at these scales. If contact point measurement of a local tip is expected to provide the best spatial resolution, the fundamental aspect of the interaction between the probe tip and the sample remains the key point on which any quantitative measurement relies. We focus on the calibration procedure that will allow measuring the thermal response (error) of a contact probe used for temperature measurement on a surface. For this purpose, a micro-hotplate made of platinum heater suspended on thin silicon nitride (SiN) membrane represents an interesting tool. The objective is to develop heated reference samples with localized temperature sensors embedded on its surface to probe the temperature during the probe contact. We report on the thermal design of low-power calibration chip and the first results obtained when contacting wire based micro-thermocouple Scanning Thermal Microscope (SThM) probes.

## 1 Problematic

In order to monitor and calibrate the SThM probe/surface interactions in temperature measurement mode, active calibration samples are required. The calibration methodology was already presented using standard hotplates not specifically designed for that purpose [1]. We report here on optimized devices with low power consumption and integrated temperature sensor to precisely adjust and measure temperature on a localized area on which the probe tip is put in contact. Although a contact area remains quasi-punctual (some tens of nanometers square), the resulting thermal perturbation area is much larger so that a resistance temperature detector (RTD) is a possible mean to directly derive the temperature of a perturbed area below the probe tip.

Figure 1 presents the temperature disturbance area on a platinum heater similar to the present device when a micro-thermocouple tip is on contact [2]. It is clear that the perturbed area is much larger than the contact point, a typical diameter of 10  $\mu\text{m}$  being relevant for insuring a local temperature measurement.

During the contact, different temperatures are involved due to the heat sink effect of the probe and the different thermal resistances encountered. Figure 2 depicts the thermal configuration of a general case of a contacting probe on a thin device such as a suspended membrane. According to the heat flux that is dissipated from the surface to ambient through the tip, one can define three thermal resistances including the probe itself ( $R_c$ ), the tip-to-surface contact ( $R_c$ ) and the surface disturbance effect ( $R_m$ ) which is analogous to the usual macroconstriction effect [1].

Consequently, during the measurement, any probe provides a value that relies on its own characteristics ( $R_c$ ), on the surface nature ( $R_m$ ), but also on the coupled effects of the tip-to-surface topography ( $R_c$ ) in which the contact

strength may have a role and the environment (vacuum, ambient etc...).

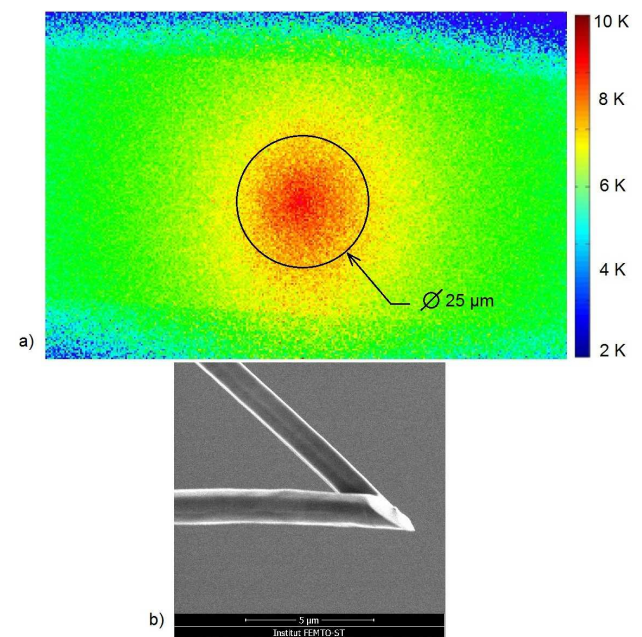


Figure 1. Surface temperature disturbance (a) obtained by subtracting near-infrared thermographs before and during the contact of a 1.3  $\mu\text{m}$  wire thermocouple probe (b). The sample is a platinum film deposited on a silicon nitride membrane (see below).

This makes a contact measurement really hard to implement and a calibration procedure one of the key points for improving present techniques of SThM. The development of calibration devices represents a first step toward this objective. The idea is to measure the “true” surface temperature, with or without contact. The direct comparison of these values, in addition to ambient and the probe itself, lead to relevant ratio that characterizes the “quality” of the sensor.

As shown in Figure 2, the main ratio is given by  $\tau$ , the “probe thermal response” as a global parameter including the three mentioned effects.

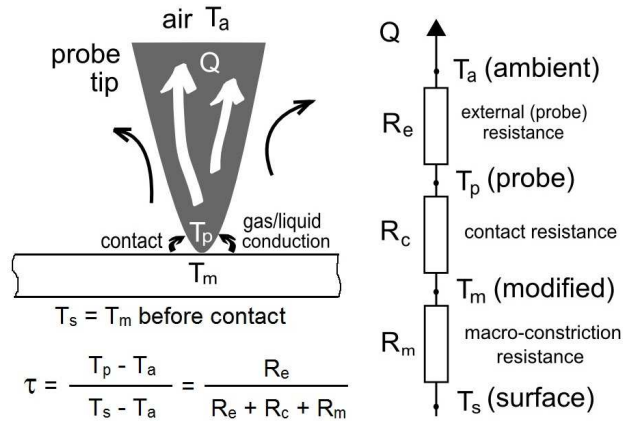


Figure 2. Thermal configuration of a contacting probe on a thin surface, dissipating a heat flow noted  $Q$  from the surface to ambient.

One can also use a ratio that is less depending on the surface nature:  $\phi = R_c/R_e$  that should ideally tend to zero for a perfect temperature sensor [3]. It is interesting to notice that these ratios are given by the measured temperatures whereas the heat flux  $Q$  is more difficult to extract. This could however lead to the knowledge of the resistance values which remains a further objective.

## 2 Experimental setup

### 2.1 Electrothermal device

Figure 3 presents the measurement principle, taking into account the SThM probe and the local temperature sensor (Figure 3a). The electrothermal device is composed of a thin insulating membrane of silicon nitride ( $2 \times 500$  nm thick) in which both platinum heater and resistance temperature detectors (RTD) are embedded. The platinum heater (150 nm thick) generates a hot central area by Joule effect whereas two symmetrically located RTDs provide their local temperature (50 nm thick). According to Figure 2, RTD values provide  $T_s$  and  $T_m$  before and during SThM tip contact respectively.

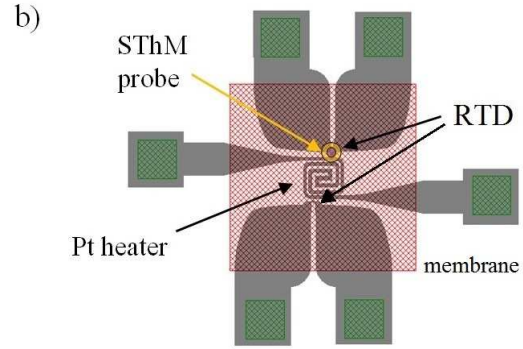
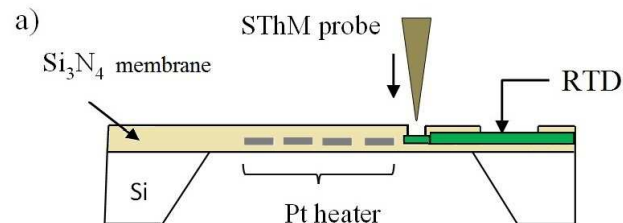


Figure 3. a) Side view, b) Top view of the device integrating a local temperature sensor on the hotplate suspended membrane.

Figure 4 presents a closer view of the central heater (Fig. 4a) and the RTD patterned using e-beam lithography (Fig. 4b) for which the sensing area is  $10 \times 10 \mu\text{m}^2$ . Fabricated devices have been characterized by determining experimentally the temperature coefficient of the resistive elements and by measuring temperature evolution with respect to hotplate power consumption. Different RTD geometry and fabrication techniques have been tested but only e-beam RTD results are presented in this article.

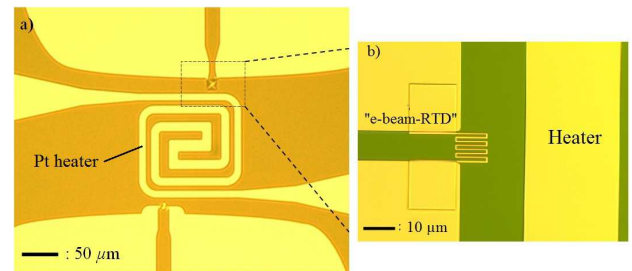


Figure 4: a) Images of low-power Joule heater with RTDs; b) example of e-beam lithography RTD geometry.

The temperature dependence of the different heaters and RTDs implemented has been measured. A climatic chamber has been used to measure the resistance variation between 30 and 200°C. The temperature coefficient of resistance (TCR) is measured for each fabricated device. Extracted values of TCR are in the range  $2.1 \cdot 10^{-3}$  to  $2.5 \cdot 10^{-3} \text{ K}^{-1}$  for the e-beam lithography RTD whereas between  $3 \cdot 10^{-3}$  and  $3.3 \cdot 10^{-3} \text{ K}^{-1}$  for the standard lithography RTDs.

### 2.2 Temperature probes

For years, we have developed and used thin wire thermoelectric couples as local temperature probes for SThM applications [1,4]. Wollaston wires (Platinum and Platinum-10% Rhodium) are used to provide a S type junction obtained by a sparking technique. Different diameters can be used, mainly  $5 \mu\text{m}$  and  $1.3 \mu\text{m}$ . Furthermore, the obtained junction can be etched using a Focused Ion Beam (FIB) to insure a reproducible tip shape as shown in the Figure 5. Figure 5a presents a  $5 \mu\text{m}$  junction and Figure 5b depicts the  $1.3 \mu\text{m}$  junction after FIB etching.

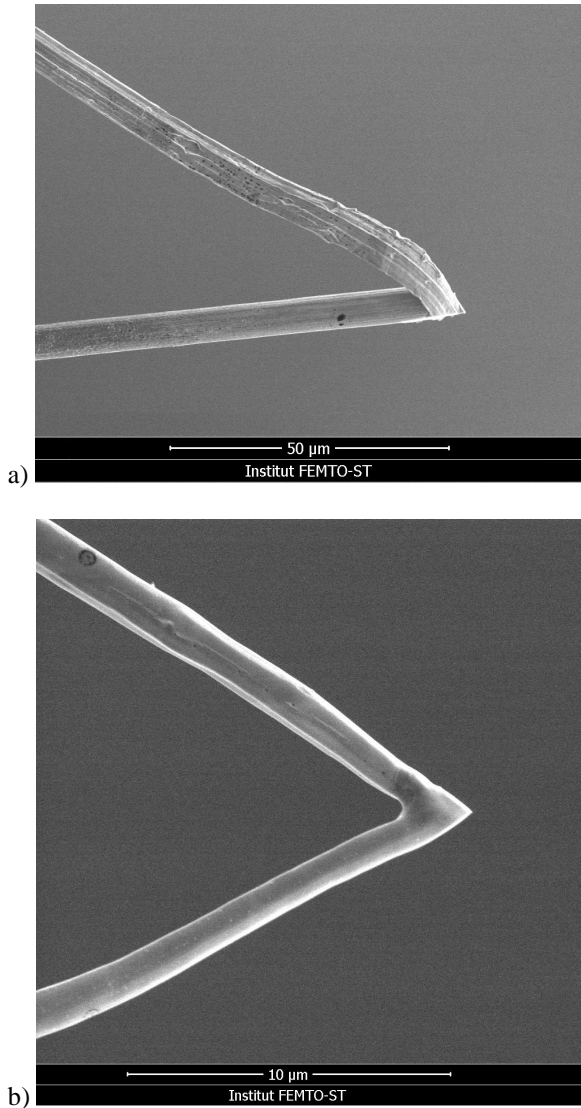


Figure 5. Thermocouple junction aspect after FIB etching; a) 5  $\mu\text{m}$  probe and b) 1.3  $\mu\text{m}$  probe.

For SThM applications, these micro-thermocouples are embedded on a tuning fork resonator so that the point contact is easily detected [5].

### 2.3 Simulation and test

Electrothermal devices (calibration chip) are stemming from usual micro-hotplate designs [6]. Their main interest in the objective of calibration system relies on an easily tunable temperature at a very low consumption level. In their development, ComsolMultiphysics® simulations are used to optimize the geometry of the heater and the position of the RTDs. In parallel, main thermophysical parameters are adjusted regarding experimental measurements obtained with our thermocouple probes. Figure 6 presents a typical result of simulation, compared with thermocouple probe measurements. A top view of surface temperature is shown in Figure 6a while the supplied power is 25 mW. The central temperature reaches 290°C as confirmed by local measurements presented in the Figure 6b. Transverse scans have also been performed with a 1.3  $\mu\text{m}$  thermocouple probe following the dashed white line of Figure 6a. Results are depicted in Figure 6c for three different powers.

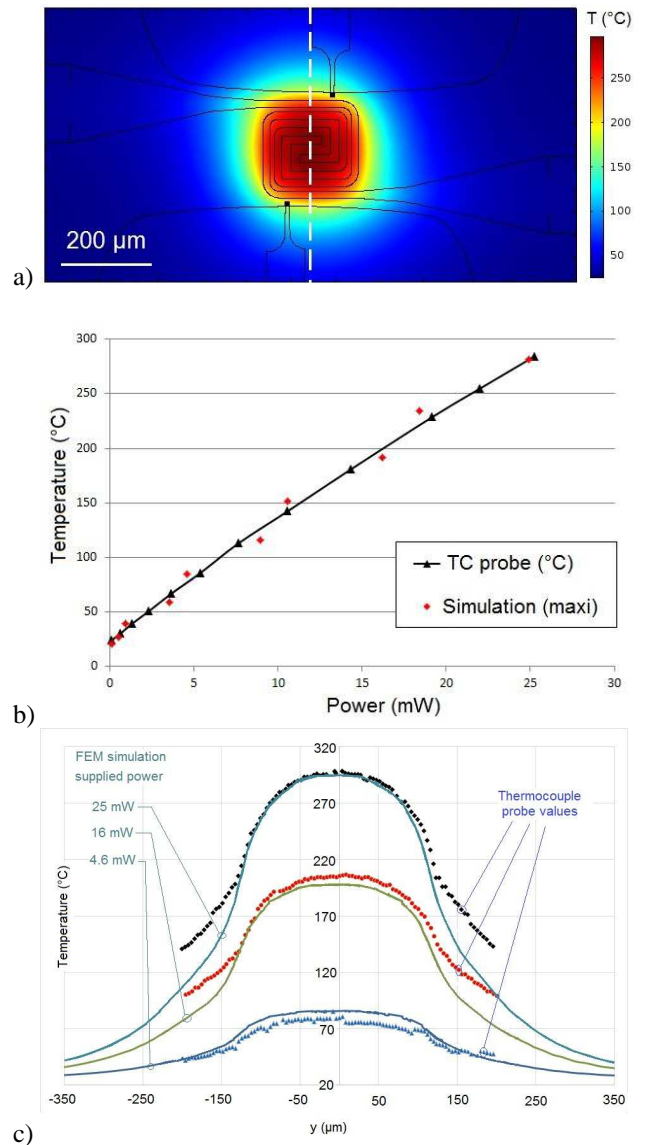


Figure 6. Comparison of simulations and measurements; a) Top view of Comsol simulation at 25 mW, b) simulated and measured central temperature versus power, and c) lateral profiles at different powers. Measurements are obtained with a 1.3  $\mu\text{m}$  thermocouple probe (see Figure 5b).

Central temperature distributions versus the heater power are in good agreement but quite dissimilar around the membrane limit. This is due to the simplified approach of the modeling. Indeed, to decrease the computing time and the required memory capacity, only the membrane has been taken into account. In these simulations, the membrane thermal conductivity is supposed as  $20 \text{ Wm}^{-1}\text{K}^{-1}$  whereas the platinum heater and RTD are supposed to be identical to bulk material (thermal conductivity of  $72 \text{ Wm}^{-1}\text{K}^{-1}$ ). The dissipation of the generated Joule heating is mainly due to the external global constant coefficient fixed to  $1000 \text{ Wm}^{-2}\text{K}^{-1}$  above and below the membrane. These values have to be discussed. However, complementary measurements and simulations will be performed in order to improve the reliability of this approach, including the effect of the contacting probe tip.

### 3 First results of calibration principle

Functionality of the calibration chip was validated with coupled SThM and RTD temperature measurements. Measurements have been performed at different supplied power and the resulting points led to fitted curves as shown in the Figure 7. Figure 7a presents a micrograph of a 5  $\mu\text{m}$  TC probe approaching the RTD area (right side). Figure 7b and 7c present the extracted curves from the measurement points of the 5  $\mu\text{m}$  and 1.3  $\mu\text{m}$  probe respectively. From these curves and knowing the ambient temperature, one can easily calculate the thermal response  $\tau$  of both probes, and their ratio  $\phi$ . It is interesting to notice the difference between the two probes due to their size. A perfect probe would indicate a thermal response equal to 1 whereas a  $\phi$  ratio near zero.

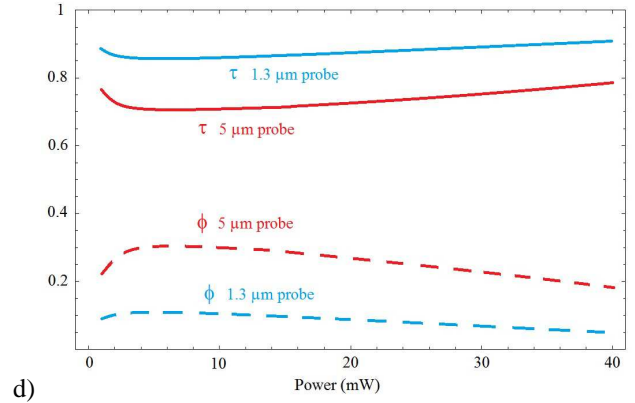
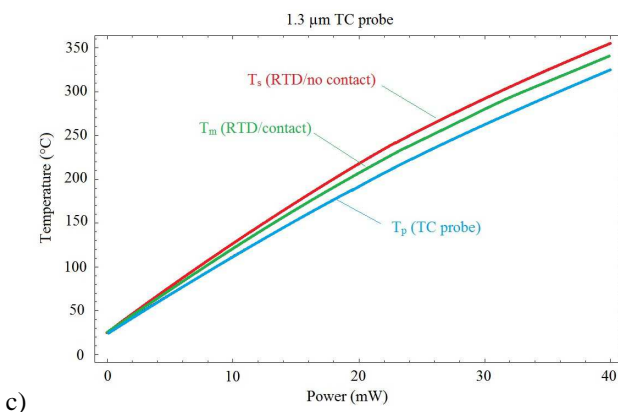
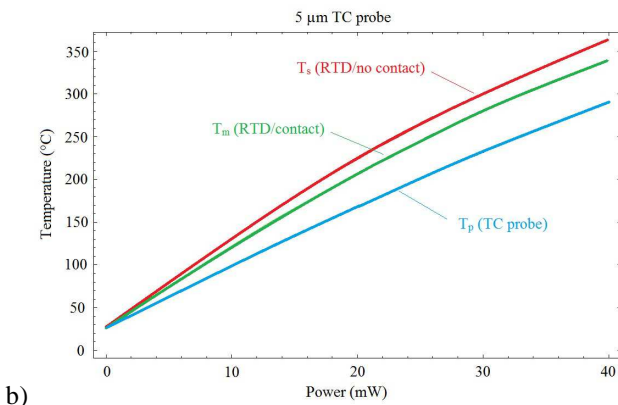
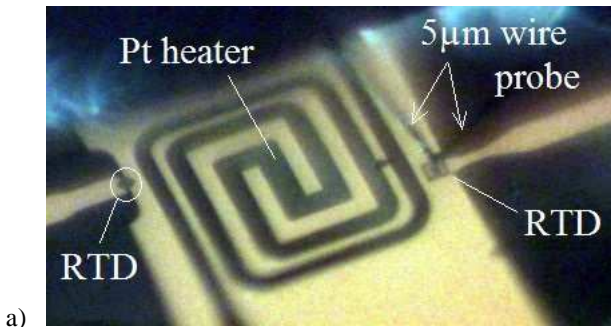


Figure 7. Experimental results: a) 5  $\mu\text{m}$  TC probe near contact RTD area; b) 5  $\mu\text{m}$  probe results; c) 1.3  $\mu\text{m}$  results; d) Extracted values of  $\tau$  and  $\phi$  for both probes.

Among the series of measurements already made, the different 5  $\mu\text{m}$  probes led to similar values whereas the 1.3  $\mu\text{m}$  exhibits large variations that can be due to the uncertainty on its actual location regarding the RTD.

Another point that can be relevant to extract, is the heat power disturbance due to the presence of the probe on the calibration device. Figure 8 depicts a comparison between the two tested probes. This is the difference between the heater Joule power supplied with and without contact at the same RTD temperature.

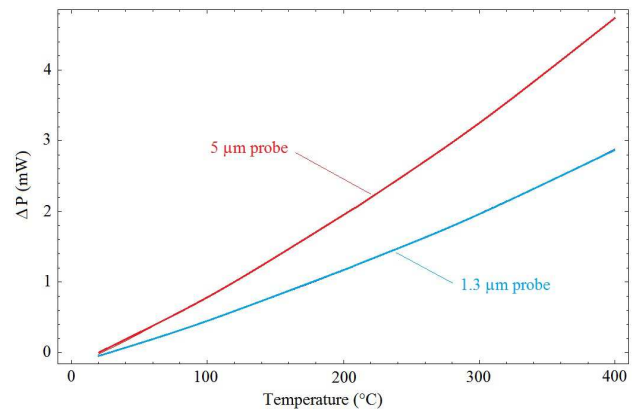


Figure 8. Disturbance power of both probes regarding surface RTD temperature.

This power difference does not corresponds exactly to the dissipated power  $Q$  mentioned above since the device thermal balance should be mastered to be strictly identical before and during the probe contact. However, this is a clear indication of the degree of disturbance of a probe.

### 4 Conclusion

These first results demonstrate the interest to use a micro-hotplate as a calibration device for SThM probes in mode of temperature measurements. The major interest is that a single measurement while contacting the probe at a given power is able to provide the thermal response of the probe or its ratio  $\phi$  which represent important calibration parameters. Different designs of chips are being tested with different measurement configurations and RTD

sensors. First results show that the variability obtained when using the smallest probes (1.3  $\mu\text{m}$  thermocouple) needs to be studied. It may simply be related to the difficulty to precisely locate the tip on the RTD sensor, or the inadequacy between their respective thermal contact areas. Improvements of simulations, including the probe contact may help to clarify this aspect.

### Acknowledgements

This work has received funding from the European Union Seventh Framework Program FP7-NMP-2013-LARGE-7 under GA N°604668 Project “QUANTIHEAT”.

### Literature

- [1] L. Thiery, S. Toullier, D. Teyssieux and D. Briand, “*Thermal contact calibration between a thermocouple probe and a microhotplate*”, *J. Heat Transfer*, 130 (9), 091601 (2008).
- [2] L. Thiery, D. Teyssieux, A. Bontempi, D. Briand and P. Vairac, “*Passive Thermal Contact Calibration of Thermoelectric Micro-sensors*”, Phonons and Fluctuations 3 Workshop, 21-24 May 2012, San Feliu de Guixols, Girona (Spain).
- [3] L. Shi, S. Plyasunov, A. Bachtold, P. L. McEuen and A. Majumdar, “*Scanning thermal microscopy of carbon nanotubes using batch-fabricated probes*”, *Appl. Phys Lett.* 77 (26), 4295-4297 (2000).
- [4] A. Bontempi, L. Thiery, D. Teyssieux, D. Briand and P. Vairac, “*Quantitative thermal microscopy using thermoelectric probe in passive mode*”, *Rev. Sci. Instrum.* 84, 103703 (2013).
- [5] A. Bontempi, D. Teyssieux, L. Thiery and P. Vairac, “*2 $\omega$ /3 $\omega$  SThM: improvements and perspectives*”, Eurotherm 103: Nanoscale and Microscale Heat Transfer IV, October 15-17, Lyon, France 2014.
- [6] D. Briand, A. Krauss, B. van der Schoot, U. Weimar, N. Barsan, W. Göpel and N.F. de Rooij, “*Design and Fabrication of High Temperature Micro-Hotplates for Drop-Coated Gas Sensors*”, *Sensors and Actuators B*, 68, 223-233 (2000).